

PACS numbers: 42.55.Px; 42.60.Fc; 42.60.Jf
DOI: 10.1070/QE2005v035n02ABEH002903

Papers devoted to the 250th anniversary of the Moscow State University

Injection laser with a stably scanning radiation pattern

A.S. Logginov, K.I. Plisov

***Abstract*. A model of self-lateral-mode-locking in an injection laser with a parabolic inhomogeneity of the dielectric constant of the active medium is proposed. It is shown that an appropriate choice of the pump current profile provides a stable scan of the radiation pattern. The role of the antiwaveguide parameter in the violation of the scan stability is discussed in detail. The spectrum of lateral modes is shown to split with increasing this parameter. Subgroups of satellite modes appear inside each mode, which efficiently interact with each other, resulting in periodic violation and recovery of the scan periodicity.**

Keywords: *injection lasers, radiation dynamics, lateral-mode-locking*.

1. Introduction

The investigation of mode locking in semiconductor lasers has a long history, beginning with the study of the radiation dynamics of planar, wide-contact injection lasers. A rich spectral composition of radiation from such lasers allows one to observe numerous spatially and spectrally temporal dynamic phenomena. Such studies are performed by the method of electrooptical chronography [1], which is very convenient for investigating fast processes proceeding in one-dimensional objects such as, in particular, the active region of an injection laser. Figure 1 shows the typical chronogram (time scan) of the near-field radiation pattern for a wide-contact heterolaser. Two types of processes are distinctly seen: relatively slow discrete displacements of the emitting spot within extended (tens of micrometres) parts of the active region and strictly periodic displacements of two emitting spots within a much narrower part of the active region. Note that the experimentally observed discrete movement of the emitting spot in extended regions is quasi-periodic. Sometimes it follows almost exactly the harmonic or saw-tooth law, and sometimes ceases.

At the initial stage of investigations, such effects could be treated as exotic and of no practical interest. In the last years, due to the outlook for using optical communication in the development of computers, it becomes possible to use the high-frequency discrete movements of the emitting spot of coherent radiation in devices for optical-channel commutation or in a timing-frequency master oscillator.

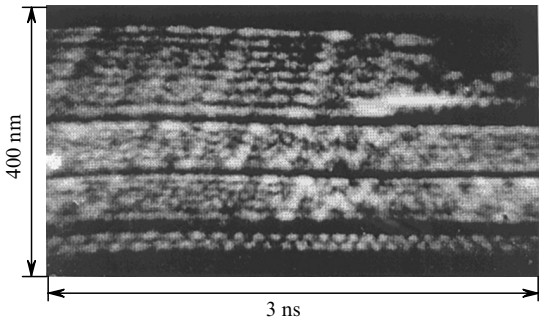

Figure 1. Chronogram of the near-field radiation of a lateral-mode-locked laser.

The periodic movement of the emitting spot along the active region of an injection laser and scanning of its radiation pattern were first observed in [2]. These effects, as well as processes that can occur under certain conditions due to excitation of the equidistant Hermite – Gaussian modes in a gas laser with parabolic mirrors [3], can be treated as the result of lateral-mode-locking. Self-lateral-mode-locking can be achieved in a laser with the Fabry – Perot resonator in the case of a parabolic profile of the dielectric constant in the active medium of the laser [4], which is equivalent to the use of parabolic mirrors.

The effect of lateral-mode-locking can be analysed by two methods. The first one is based on the solution of the rate equations [5]. This method is simple and allows a sufficiently complete analysis of the laser dynamics. The second method [6, 7] is based on a direct solution of the parabolic equation of the diffraction theory. Its main advantage is the absence of *a priori* assumptions about the initial mode composition of radiation. The lateral mode composition is determined here directly during calculations and dynamically changes together with the main parameters of the system. Both these approaches give the results in well agreement with the experimental data obtained earlier; however, the latter approach is preferable for a deeper insight into the essence of the phenomenon.

The aim of our numerical simulation of lateral-mode-locking was to find the combination of parameters at which the harmonic scan of the radiation pattern would be strictly periodic. As shown in [7], the scan periodicity is violated mainly due to the deviation of intermode spectral intervals from the equidistant spacing. The deviation from the

A.S. Logginov, K.I. Plisov Department of Physics, M.V. Lomonosov Moscow State University, Vorob'evy gory, 119992 Moscow, Russia

Received 13 September 2004
Kvantovaya Elektronika **35** (2) 111 – 115 (2005)
Translated by M.N. Sapozhnikov

equidistant mode spacing can be caused at least by two factors: the influence of the boundaries of the active strip and the inhomogeneous burning of the profile of inverted carriers by the electric field.

This paper is a continuation of the study started in [7]. We have shown that, by choosing the pump current profile sufficiently well smoothed along the lateral coordinate, we can substantially reduce the influence of inverse population burning on the emission spectrum, thereby obtaining a strictly periodic scan of the emitting spot and radiation pattern.

2. Mathematical model

Figure 2a shows schematically the structure under study. We assume that a laser of length L and width w has the active medium of width w_a and thickness d_a pumped by the current of density J. The real part of the dielectric constant along the coordinate y has a parabolic profile (Fig. 2b).

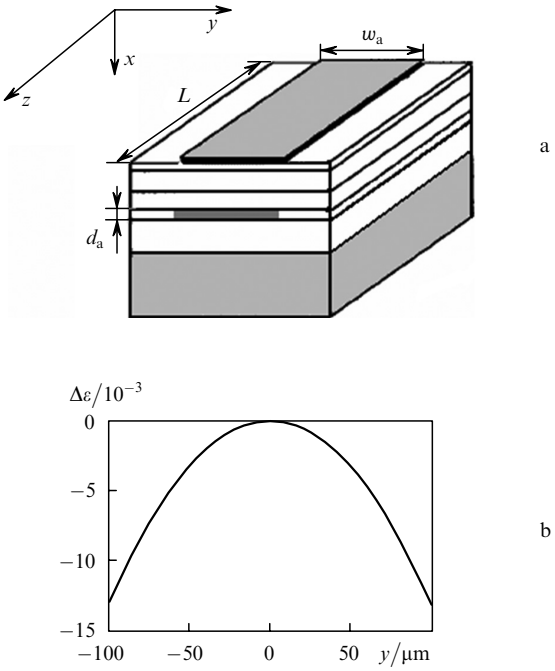

Figure 2. Scheme of a diode laser (a) and the parabolic inhomogeneity of the dielectric constant in the active region (b).

In this paper, we use the mathematical model which is described in detail in [7] and represents the beam propagation method adapted for the specific problem. The three main basic equations of the model are presented below. The optical part is described by the parabolic equation of the diffraction theory

$$\pm 2ik\,\frac{\partial\psi_{f,b}}{\partial z}+\frac{\partial^2\psi_{f,b}}{\partial y^2}+k_0^2\Gamma\Delta\varepsilon(y,z)\psi_{f,b}=0, \qquad (1)$$

where $k=k_0\bar{\eta}$; $\bar{\eta}^2=\Gamma\eta_a^2+(1+\Gamma)\eta_p^2$; $\psi_{f,b}$ are the electric fields of the forward and backward waves, respectively; $\Delta\varepsilon(y,z)$ is the contribution from all perturbations of the imaginary and real parts of the dielectric constant; k_0 is the wave number in vacuum; η is the effective refractive index; $\eta_{a,p}$ are the refractive indices of the active and passive parts, respectively; and Γ is the optical confinement factor.

We assume, as usual, that the distribution of the dielectric constant ε in the direction x (Fig. 2) experiences a jump in the active region, resulting in the formation of a waveguide in this direction:

$\varepsilon(x)=\eta_a^2$ inside the active region,

$\varepsilon(x)=\eta_p^2$ in emitter layers.

The concentration of inverted carriers was calculated by solving the diffusion equation

$$\frac{\partial N}{\partial t}=\frac{J}{ed_a}+D_a\,\frac{\partial^2 N}{\partial y^2}-\frac{N}{\tau_{nr}}-\frac{\Gamma g(N)}{d_a\hbar\omega}\left(|\psi_f|^2+|\psi_b|^2\right). \qquad (2)$$

Here, N is the concentration of nonequilibrium carriers; e is the electron charge; D_a is the ambipolar diffusion coefficient; τ_{nr} is the nonradiative recombination time; $g(N)=aN-b$; a and b are coefficients characterising the contribution of nonequilibrium carriers to the gain and internal losses in the active medium, respectively; and ω is the optical radiation frequency.

The quantities in Eqn (2) are normalised so that the integral of the square of the electric-field amplitude with respect to the lateral coordinate gives power in watts if other parameters are expressed in SI units.

The influence of the concentration of inverted carriers and the parabolic profile of the refractive index on the electric field is taken into account in the coefficient $\Delta\varepsilon$:

$$\Delta\varepsilon=-\eta_a^2\,\frac{y^2}{s^2}+a\eta_a\,\frac{RN}{k_0}+\mathrm{i}\,\frac{\eta_a}{k_0}\,(aN-b)$$

$$-\mathrm{i}\,\frac{\eta_a}{k_0}(1-\Gamma)\frac{\alpha_p}{\Gamma}, \qquad (3)$$

where s is the coefficient of parabolic inhomogeneity of the refractive index; R is antiwaveguide parameter; and α_p is the coefficient of losses in passive regions.

Equation (1) was solved by the method of multiple propagation of radiation in the active medium. Because of the burning of inverted carriers by the electromagnetic fields of the forward and backward waves, the inversion distribution was recalculated using Eqn (2) after each round trip in the resonator.

The main advantage of this model is that the mode composition of radiation is calculated directly from boundary conditions in the form of the profile of nonequilibrium carriers. The profile itself 'breathes' together with variations in the electric-field amplitude. This means that the spectral composition of radiation does not remain constant. The recalculation of the concentration of nonequilibrium carriers after each round trip of radiation in the resonator and consideration of the corresponding variations in the perturbation of the dielectric constant allow one, in turn, to introduce corrections to the electric-field distribution.

The rate equation model [5] takes into account continuous variations in the profile of nonequilibrium carriers only in the perturbation of the eigenvalues of the resonator modes, whereas the modes themselves are assumed invariable. This is quite justified when the dielectric constant changes weakly, because the perturbation of eigenfunctions in this case has a higher order of smallness than the

perturbation of the eigenvalues. However, as the inhomogeneity of the dielectric constant profile increases, this approach is no longer adequate.

3. Results

As shown in [7], the deviation from the equidistant mode spacing is mainly caused by the boundaries of the active region and the perturbation of the profile of nonequilibrium carriers. The latter is always present and cannot be completely eliminated.

The width of the active region determines the number of modes which can be amplified to produce lasing. The properly selected parabolic inhomogeneity profile can provide the formation of generated modes mainly due to this profile rather than due to the influence of the active-region boundaries.

The magnitude of contribution of the profile of nonequilibrium carriers to the spectrum of generated modes is mainly determined by the antiwaveguide parameter. However, even in the hypothetical situation of the zero antiwaveguide parameter, nonequilibrium carriers will contribute to the mode profile and eigenvalues because the imaginary part of the dielectric constant is also involved in the formation of the mode spectrum.

The numerical calculation shows that even when $R = 0$ in the case of the square injection current profile only somewhat smoothed by diffusion, it is impossible to obtain stable scanning (the calculation parameters are presented below). In this case, the burnt profile of nonequilibrium carriers has the form presented in Fig. 3.

Radiation wavelength $\lambda/\mu m$	0.82
Resonator length $L/\mu m$	300
Resonator width $w/\mu m$	200
Active strip width $w_a/\mu m$	75
Total width of active layers $d_a/\mu m$	0.06
Reflectivity R_1 of the highly reflecting mirror	1
Reflectivity R_2 of the output mirror	0.9
Refractive index η_a of the active region	3.6
Refractive index η_p of passive regions	3.3
Optical confinement factor Γ	0.1
Effective group refractive index η_g	3.4
Antiwaveguide parameter R	0–1.4
Coefficient of parabolic inhomogeneity s/cm	0.315
Gain parameter a/cm^2	1.5×10^{-15}
Gain parameter b/cm^{-1}	150
Nonresonant waveguide losses in passive regions α_p/cm^{-1}	10
Lifetime of carriers τ_{nr}/ns	1
Pump current density $J/A\ cm^{-2}$	170
Ambipolar diffusion coefficient $D_a/cm^2\ s^{-1}$	33

First we explained our failure to obtain stable scanning by an incomplete recovery of the burnt profile of nonequilibrium carriers to the instant of the next appearance of a bright spot. It is obvious that the profile burning would not affect radiation at all if diffusion had time to smooth the inversion profile for the time of the order of the scan period. To verify this assumption, we performed numerical calculations for the diffusion coefficient exceeding the real coefficient by an order of magnitude. The aim was to find out whether it is possible in principle to achieve a strictly periodic scanning regime.

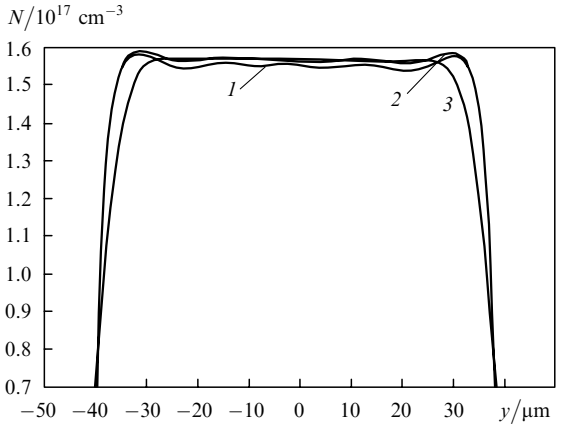

Figure 3. Smoothing of the burnt profile of the inverse population by diffusion: the profile immediately after burning (*1*) and after the scan half-period for $D_a = 33$ (*2*) and 300 cm^2 s^{-1} (*3*).

The calculation showed that for such a large diffusion coefficient, scanning remains periodic during the observation time. A comparison of the concentration profiles for injected carriers at substantially different diffusion coefficients ($D_a = 33$ and 300 cm^2 s^{-1}) (Fig. 3) shows that the difference in the concentration profiles in the central part of the active region is small. Of course, in the case of a large diffusion coefficient, the inversion profile in the central part is smoother; however, the difference in the carrier concentrations in this region is negligibly small compared to that near the boundaries of the active region. Here, in the case of a small diffusion coefficient, a noticeable difference between the concentrations of nonequilibrium carriers is observed. In the case of a large diffusion coefficient, nothing of this kind happened. This suggests that, when the width of the active region is large enough, the radiation modes become nonequidistant mainly due to the edge inhomogeneity of the concentration profile of injected carriers.

The calculation shows that the diffusion coefficient exceeding the real coefficient by an order of magnitude is insufficient to smooth completely the inversion profile at the times of the order of the scan period. Because the difference between the large and small diffusion coefficients plays an insignificant role in the central part of the inversion profile, it is reasonable to use the smoothed pump current profile together with the real diffusion coefficient. In this case, we can produce the distribution of carrier concentration at the boundaries of the active region as in the case of a large diffusion coefficient.

To form the smoothed pump current profile, we determined the stationary distribution of the concentration of nonequilibrium carriers obtained by solving the diffusion equation with the diffusion coefficient exceeding the real coefficient by an order of magnitude. The calculated concentration profile was normalised to the maximum of the pump current amplitude. As a result, we obtained the smoothed pump current profile which can be directly used for simulating processes proceeding in the laser. By using this profile, we realised a completely stable scan of the emitting spot over the laser end face for the case of four locked modes, the standard diffusion coefficient, and the antiwaveguide parameter $R = 1$ (Fig. 4).

To determine the influence of the antiwaveguide parameter on the behaviour of the mode-locked laser, we performed

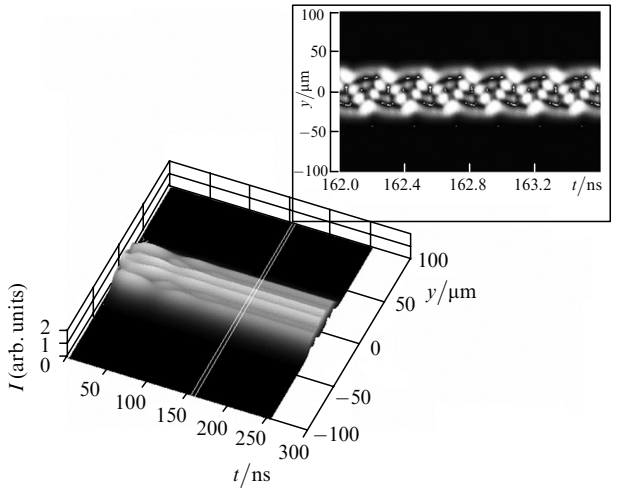

Figure 4. Calculated chronogram of the near-field radiation I. Passage to a stable scan regime involving four modes for the standard diffusion coefficient and $R = 1$.

a series of numerical experiments by varying the value of the parameter, the rest of the parameters being fixed. We found that the scan periodicity was most stable for small values of the antiwaveguide parameter $R = 0 - 1$. As the antiwaveguide parameter increased, the passage to a stable scanning slowed down, and finally periodically repeated beats appeared, when scanning was observed only during a certain time interval, then disappeared for some time and recovered again.

The reasons for such a spatiotemporal behaviour of the laser can be conveniently analysed by considering the evolution of the emission spectrum depending on the antiwaveguide parameter. One can see from Fig. 5 that the calculated spectrum of modes splits with increasing R and the amplitude of satellites of split modes increases. This means that the contribution of energy transfer between the satellites of one mode to the total dynamics gradually increases. The frequency splitting also gradually increases. When $R = 0$, the splitting of the mode spectrum is absent (Fig. 5a). However, already for $R = 0.6$, the splitting can be observed at times of 200 ns (Fig. 5b), while for $R = 1.4$, the satellite amplitude is equal to almost half the amplitude of the initial mode (Fig. 5c).

The scan stability is violated mainly due to the splitting of the mode spectrum. The splitting appears due to the influence of inhomogeneities of the inversion population profile on the mode composition of radiation. The increase in the antiwaveguide parameter is inevitably accompanied by the increase in the contribution of the profile inhomogeneity to the spectral composition of radiation. The lateral modes of the laser, still remaining Hermite–Gaussian polynomials, rearrange their eigenvalues spectrum in response to the perturbation of the initially specified refractive index profile. One of the satellites is enhanced after mode splitting. As a result, the satellites of adjacent modes can be non-equidistant. After splitting, the satellites of each of the modes strongly interact with each other due to their identical profiles. Energy transfer at the split frequency causes the rearrangement of the spatial distribution of radiation in the near-field chronogram.

Therefore, because of the almost total orthogonality of the mode profiles, no interaction can occur between the modes. All the processes related to the deviation from a sinusoidal scan are caused by the interaction between the generating mode and its satellites, whose profiles are completely overlapped. This conclusion is confirmed by almost complete absence of beats in the solution of a system of rate equations in paper [5], where the satellites of modes could not exist because this model uses the preliminary specified spectral composition of radiation. Weak beats obtained in [5] can be explained by the incomplete orthogonality of the modes resulting in their interaction. During the interaction between different lateral modes, the radiation pattern changes much weakly than upon the interaction between their satellites.

The study of the splitting of the mode spectrum showed that the splitting value does coincide with the non-equidistance in the spectrum: if $\Delta\omega$ is the splitting value and T_b is the beat period, $T_b = (\Delta\omega)^{-1}$ with good accuracy. Of course, such a simple relation takes place when only one of the modes is predominantly split. As the antiwaveguide parameter increases, the frequency detuning of satellites increases and, hence, the beat frequency also increases.

4. Conclusions

We have shown that the use of the smoothed current profile provides a stable scan of the radiation pattern of a wide-

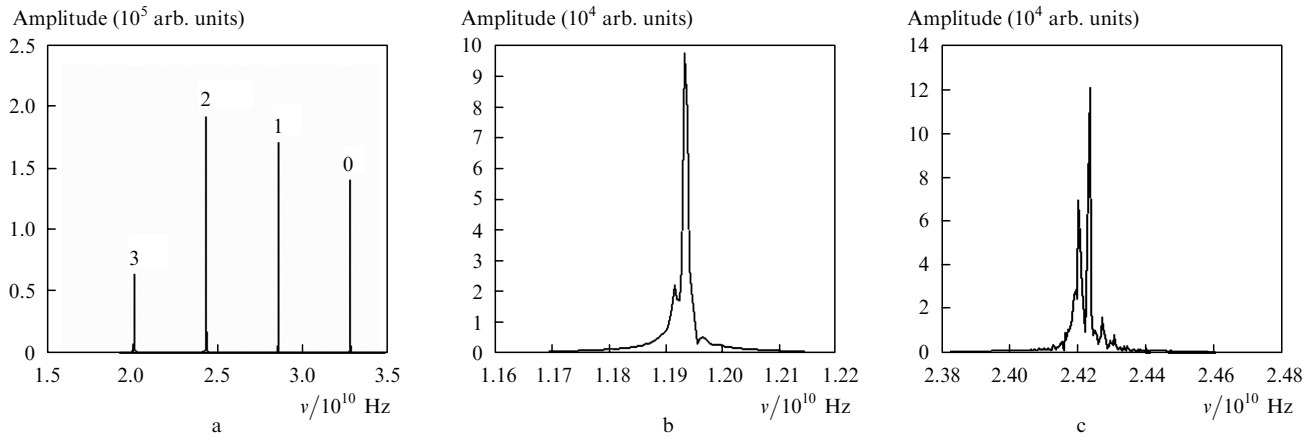

Figure 5. Calculated spectra of lateral radiation modes for $R = 0$ (a), 0.6 (b), and 1.4 (c).

contact injection laser. The study of the role of the antiwaveguide parameter in the violation of the scan stability has shown that the spectrum of generated lateral modes splits with increasing this parameter. Satellites appear for each of the modes, which efficiently interact with each other, resulting in the periodic violation and recovery of the scan regime. It is shown that the amplitudes and detunings of satellites increase with increasing the antiwaveguide parameter. As a result, the scan regime becomes unstable and beats appear which are manifested in successive disappearance and appearance of the scan periodicity.

References

1. Miller D.A.B. *Proc. IEEE.*, **8** (6), 728 (2000).
2. Butslov M.M., Stepanov B.M., Fanchenko S.D. *Elektronno-opticheskie preobrazovateli i ikh primenenie v nauchnykh issledovaniyakh* (Electrooptical Converters and Their Application in Scientific Research) (Moscow: Nauka, 1978).
3. Auston D.H. *IEEE J. Quantum Electron.*, 4, 420 (1968).
4. Kurylev V.V., Logginov A.S., Senatorov K.Ya. *Pis'ma Zh. Tekh. Fiz.*, **8**, 317 (1968).
5. Logginov A.S., Plisov K.I. *Laser Phys.*, **14**, 1105 (2004).
6. Logginov A.S., Plisov K.I. *Kvantovaya Elektron.*, 32, 553 (2002) [*Quantum Electron.*, 32, 553 (2002)].
7. Logginov A.S., Plisov K.I. *Kvantovaya Elektron.*, 34, 833 (2004) [*Quantum Electron.*, **34**, 833 (2004)].